Measurement of the Interfacial Shear Strength of a PEO Coated Aluminium Alloy

D. T. Asquith*, Y. H. Tai*, C. X. Wong* J. R. Yates*, A. Matthews†, and A. L. Yerokhin†

*SIRIUS, Department of Mechanical Engineering, University of Sheffield
Mappin Street, Sheffield S1 3JD, UK

†RCSE, Department of Engineering Materials, University of Sheffield
Mappin Street, Sheffield S1 3JD

d.asquith@sheffield.ac.uk

Keywords: Interfacial shear, optical techniques, PEO, and aluminium

Abstract. Interest in oxide ceramic coated metals, in particular aluminium alloys has increased in recent years. Treatment processes such as plasma electrolytic oxidation (PEO) are more frequently being exploited commercially to provide hard wearing chemical and thermal barriers. This has led to an interest in the failure of such coated systems and the development of duplex systems, those using mechanical pre-stressing, for increased fatigue life. Failure mechanisms in these systems are often assumed without testing thus limiting our ability to optimise. The influence of interfacial shear strength is crucial to the understanding of the failure mechanism in both simple treatments and duplex systems. This paper demonstrates a method for evaluating the interfacial shear strength in PEO coated 2024 as part of a simple tensile test. Direct optical methods have been used to measure surface strains at macro and micro scales and the shear lag method applied to infer the interfacial bond strength. The influence of coating on the general stress-strain behaviour is examined and the interfacial shear strength evaluated.

Introduction

The application of lightweight materials such as aluminium to structures continually challenges engineers to improve characteristics in both bulk and surface properties. Plasma Electrolytic Oxidation (PEO) is a relatively young technique which can be used to provide a hard ceramic coating which is resistant to thermal, electrical and chemical attack. Predominantly so far PEO has been limited to non strength critical applications as the process has a tendency to substantial reduce the fatigue resistance of the substrate. It has been demonstrated that prior cold-work can significantly recover the loss in fatigue performance due to PEO treatment [1] but a basic understanding of the failure process still eludes us.

Failure of coatings can be broadly fitted into two categories: de-lamination, where the coating spalls away from the substrate and brittle fracture, where the coating cracks eventually forming a crazed pattern. In the case of PEO coatings on aluminium the latter situation of brittle fracture can be considered to introduce a pre-crack into the substrate accelerating failure whilst de-lamination has less of an influence. The coating failure mechanism therefore has a significant influence over the overall failure of a treated component subjected to loading. This mechanism can be considered to be a function of the bond strength between coating and substrate which in turn can be characterised by the interfacial shear strength. It is also important to consider that a coating susceptible to de-lamination is likely to perform poorly in terms of wear resistance and a poor bond will result in reduced durability for other protective characteristics.

To fully exploit the capacity of PEO coatings in structural applications it is necessary to optimise the coating behaviour and to do this we require a means of characterising the failure mechanisms. Interfacial shear strength has been measured previously in idealised situations for thin films and has been demonstrated to be a good indicator of bond strength [2]. In this paper the technique has been

further developed and applied to a simple tensile test measured in real time using a combination of low and high magnification direct optical techniques.

Experimental Work

Specimens

Flat tensile specimens were prepared from AA2024-T3 to ASTM E8M with the addition of a threaded hole in one end to allow an electrical contact for PEO coating. Specimens were then polished to 1000 grit and de-greased prior to coating. PEO treatment was performed in a dilute alkaline electrolyte with additions of 2-3g.l^{-1} Na_2SiO_3 and $Na_3P_2O_7$ [3]. A pulsed bipolar current supply was used with frequency set at 2kHz and current ≈ 30A.dm^{-2}. Specimens were suspended by a threaded contact insulated from the electrolyte with a plastic jacket so as to provide PEO treatment to the entire specimen surface. Treatment was conducted at a maintained temperature of 30°C for 30minutes with a growth rate of approximately 1μm per minute.

Imaging system and DIC

The imaging system used for this work consisted of a complete DIC system and computer controlled digital SLR camera which were synchronised by correlating the load data from the test machine. The DIC system allowed for good quality images to be taken at 40× magnification at a rate of up to 6.0 Hz but for the purpose of this work, an acquisition rate of 2.0 Hz sufficed. Set-up of the camera and lenses consisted of a 2.0 million pixel monochrome CMOS camera, machine vision lenses providing 0.7x to 4x magnification, 5× objective lens and suitable fibre optic lighting. This gave sufficient resolution to identify cracks forming on the surface of the specimen. No image correlation was carried out on the images obtained because of the current inability of the system to track a given area. Calibration was carried using a 12μm Vickers indent on a block.

For image correlation purposes to obtain displacement data for generating associated stress strain curves, the digital SLR system was used. This consisted of a digital SLR camera with a macro lens triggered by a computer to take an image every 3 seconds synchronised with the load which was sufficient to give good images for correlation. Images of the fracture process were then extracted and processed using commercial DIC software supplied by LA Vision. Accuracy of DIC has been shown by previous work to be very good [4].

In order for digital image correlation to be carried out, a random pattern was needed on the surface of the specimen. This was achieved by lightly spraying one side of the specimen with a combination of white and black acrylic based paint. Combined with the gray coloured surface as a result of the PEO coating, good resolution for DIC was achieved. The resultant speckle pattern can be seen in Figure 1 and the experimental set-up is shown in Figure 1.

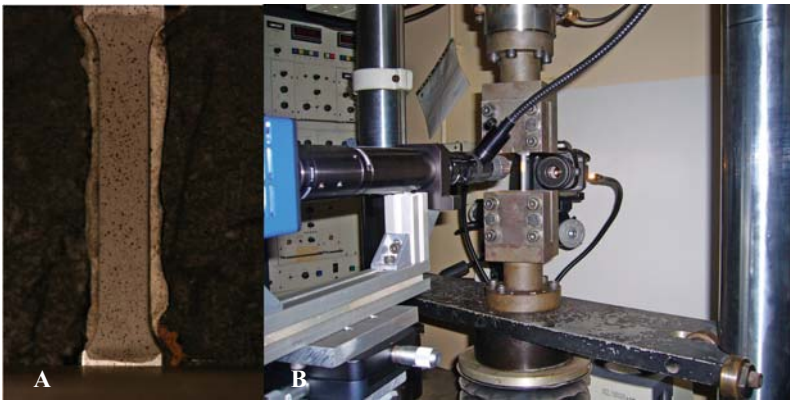

Figure 1 A – Speckle pattern used for DIC and B – Experimental setup showing machine vision system and dSLR.

Interfacial Shear Strength

Interfacial shear strength was measured using the shear lag model developed by Agrawal and Raj [5] and further refined by Ollivier [2]. The principal of shear lag relies on the support of a tensile load from substrate to coating through the bond layer. As the specimen is loaded in tension a shear stress (τ) develops between the substrate and coating, the shear stress produces a tensile stress in the coating. At a sufficient load (σ_f) the coating begins to crack as the induced load exceeds the tensile strength of the coating. At first this is manifested as random cracks but rapidly develops to parallel cracks perpendicular to the load direction. The separation of these cracks, λ, is therefore related to the fracture strength of the coating and the interfacial shear stress. Based on a sinusoidal shear stress distribution Agrawal and Raj [5] identified the location of new cracks with increasing load to be at the point of maximum coating tension which lies at approximately $\lambda/2$. This is illustrated in Figure 2.

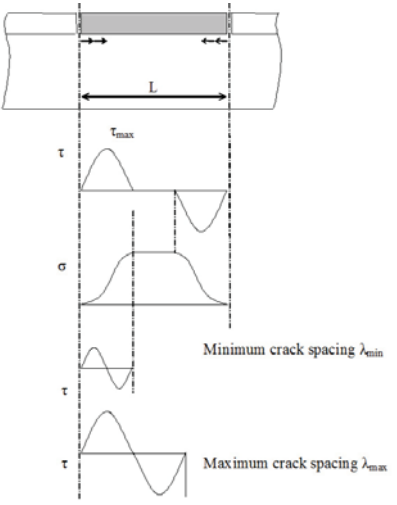

Figure 2 Formation of cracks as a result of load transferred through the interface and relationship between maximum and minimum crack lengths.

From this it can be assumed that the cracks will be distributed bi-normally with maximum and minimum crack spacing of λ_{max} and λ_{min} linked by the equation:

$$\lambda_{min} = \lambda_{max} / 2 \qquad \text{Eqn. 1.}$$

The relationship between crack spacing and interfacial shear strength is taken from [5] and defied as:

$$\tau_{max} = \frac{\pi t}{\lambda_{max}} \sigma_{fracture} \qquad \text{Eqn. 2.}$$

Where t is the coating thickness and $\sigma_{fracture}$ is the fracture stress of the coating, this is derived from the applied strain during testing at which the first random cracks appear and related by the equation:

$$\sigma_{fracture} = E\varepsilon_{fracture} \qquad \text{Eqn. 3.}$$

Young's modulus for the coating (E) can be obtained from the literature for nano-indentation measurements on similar coatings [6].

Crack Separation Measurements

The imaging process produces a substantial amount of data in the form of digital images, to demonstrate the viability of the technique only a small number of these need analysing. A number of suitable images exhibiting midpoint cracking were selected manually and visual edge detection conducted by tracing the cracks on the images using a digital graphics tablet, with a pen-nib size of 2 pixels. Red lines were used as the colour stands out on the images, minimising tracing errors. Each of the pre-processed image layers were then processed by the algorithm as described below:

1. Convert the RGB image to a black and white image (Converts all red lines to black to simplify processing).
2. Crop outer edges to remove ticks (Lines of 5 pixel width were cropped away from the right edge and the bottom edge).
3. Create a sliding window at the left edge of the image. This height of the window is the height of the image; with a specifiable horizontal width (2 pixels were selected as the window width. Longer lengths can be selected to account for missing pixels caused by tracing errors).
4. Project the black edges on that sliding window to produce a single vector column that represents the black and white pixels.
5. Measure the distances between subsequent black pixels, starting from the first black pixel encountered going down that vector column.
6. Record the distances and delete distances that are smaller than a certain threshold. This step is to simply remove adjacent black pixels that are part of a line (10 pixels were selected as the threshold).
7. If the sliding window is not at the right edge of the image, slide the window one pixel horizontally to the right and repeat steps 4 to 6.

This will create a set of crack distance measures for all the images. In order to facilitate analysis, estimates of the probability density were produced using histograms of the measurement sets. The histogram is constructed based on the equation:

$$\hat{p}(z_i) = \frac{1}{nh} \text{ (Number of datapoints in the same bin as } z_i\text{)} \qquad \text{Eqn. 4.}$$

z_i is the i^{th} datapoint, n is the number of datapoints in the measurement set and h is the width of the bins. The caret denotes an estimated quantity. The histogram demonstrates statistically that the cracks are forming in an approximately bi-normal manner, confirming that they satisfy eqn. 1. The centre of the peak for λ_{max} can be assumed to be a reasonable crack length to use for ultimate shear strength calculation.

Results

Stress vs. Strain Curves

The stress strain curves for coated and uncoated 2024-T3 are shown in Figure 3. PEO coating results in a slightly lower yield stress and strain at failure. This is most probably as a result of the introduction of defects (cracks) at the surface as a result of the coating process.

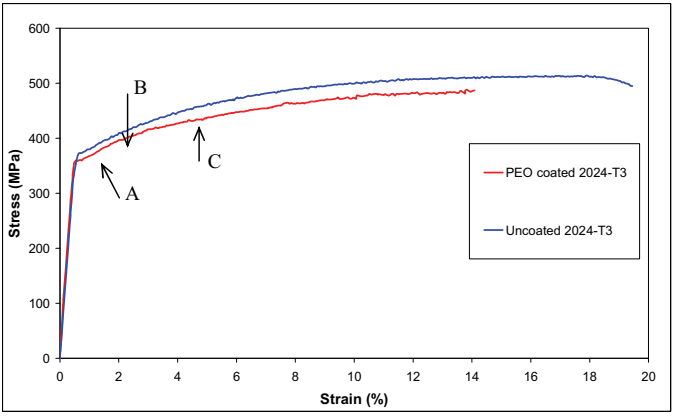

Figure 3 Stress vs. strain curves for coated and uncoated 2024-T3. Letters correspond to images shown in Figure 4.

Cracking Behaviour

Figure 4 shows three stages of cracking observed in the tensile tests. Initially, random cracks are seen and the strain at which these first appear is used to calculate the fracture stress of the coating from eqn. 3. These subsequently develop into the characteristic parallel transverse cracks which eventually exhibit the midpoint cracking phenomenon. The cracks observed here show a more random path than might be seen in some idealised situations, this is as a result of the inherent network of cracks and pores in PEO coatings [7].

However, the cracks tend to be reasonably transverse and uniformly separated and can therefore be considered representative of the shear lag model. Finally the coating begins to spall away at high strain; data collected here is currently of little experimental value. Manually processed crack layers

are also shown to aid distinction between cracks and surface morphology, in practice these were processed on higher resolution images.

Figure 5 shows a histogram of crack separation distribution in the midpoint cracking regime, a bi-normal distribution is evident and confirming that the PEO coatings exhibit shear lag behaviour. The peaks for λ_{max} and λ_{min} occur at 162μm and 81μm respectively. From this value of λ_{max} = 162μm it is possible to estimate the interfacial shear strength, this is found to be τ_{max} = 0.76 GPa. This value for τ_{max} obtained is reasonable when compared to similar results for metal ceramic interfaces found in the literature [5].

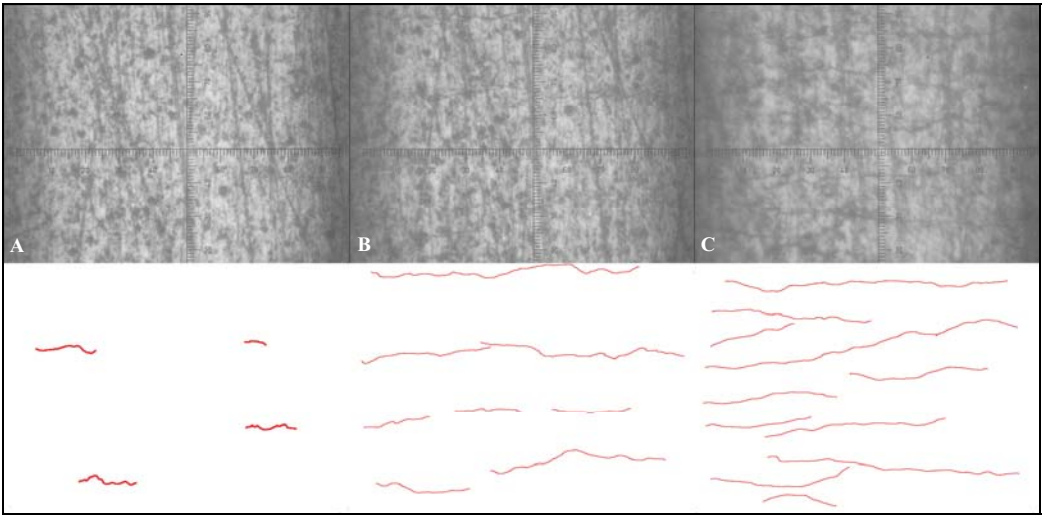

Figure 4 A – onset of random cracking at ~0.5% strain, B – Stable transverse cracks with some midpoint cracking at 1.4% strain and C beginning of spallation at 3.9% strain.

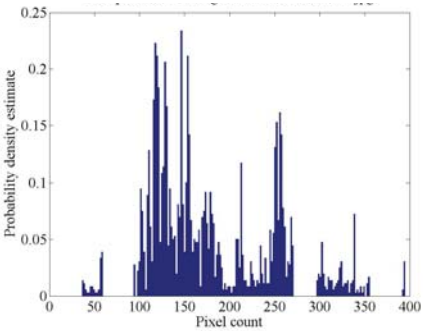

Figure 5 Histogram of crack separations taken at 2.5% strain, bi-normal distribution shows peaks at ~125pixels and 250pixels (1000pixels = 650μm)

Of particular interest to the failure of coated material is that the coating begins to crack at relatively low strain (~.5%) but remains stable up to around 4% strain due to its high bond strength. This implies that although coatings have good adhesion properties they will also initiate cracks in the substrate due to the inherent intimacy of the bond. Accelerated failure is therefore expected.

Conclusions

Interfacial shear strength has successfully been evaluated as an indication of bond strength between a PEO layer and its aluminium substrate by a non-direct optical technique using synchronous digital image correlation and digital microscopy. This technique has the benefit of using real time measurements without the requirement for electron microscopy, a single specimen can be used to provide stress strain and interfacial shear data.

Further Work

Measurements of interfacial shear strength can be made on further specimens to evaluate adhesion properties of different coating systems. This can be used to optimise process parameters to improve coating/substrate performance.

A further consideration to this work would be the incorporation of residual stresses in both the coating and substrate to the shear lag model. Though good data for substrate residual stresses exists [8] such data for the coatings is as yet unavailable.

References

(1) Asquith D T, Yerokhin A L, Yates J R, and Matthews A, *Effect of combined shot-peening and PEO treatment on the fatigue behaviour of 2024 Al alloy.* Thin Solid Films, 2006. **515**(3): p. 1187-1191.

(2) Ollivier B, Dowey S J, Young S J, and Matthews A, *Adhesion assessment of DLC films on PET using a simple tensile tester: Comparison of different theories.* Journal of Adhesion, Science and Technology, 1995. **9**(6): p. 769-784.

(3) Yerokhin A L, Shatrov A, Samsonov V, Shashkov P, Pilkington A, Leyland A, and Matthews A, *Oxide ceramic coatings on aluminium alloys produced by a pulsed bipolar plasma electrolytic oxidation process.* Surface and Coatings Technology, 2005. **199**(2-3): p. 150-157.

(4) Tai Y H, Asquith D T, and Yates J R. *Optical Characterisation of Failure Mechanics in an Aluminium-Lithium Alloy*. in *ICEI 2007*. 2007. UTeM, Malaysia

(5) Agrawal D C and Raj R, *Measurement of the Ultimate Shear Strength of a Metal-Ceramic Interface.* Acta Metall, 1989. **37**(4): p. 1265-1270.

(6) Khan R H U, Yerokhin A L, and Matthews A. *Advanced Characterisation of Plasma Electrolytic Oxidation Coatings on Aluminium: Effects of Direct Current Density and Electrolyte Concentration on Residual Stresses*. in *35th International Conference On Metallurgical Coatings And Thin Films*. 2008

(7) Curran J A and Clynne T W, *Porosity in plasma electrolytic oxide coatings.* Acta Materialia, 2006. **56**: p. 1985-1993.

(8) Asquith D T, *Residual Stress and Fatigue in Cold-Worked, Hard-Coated 2024-T351 Aluminium Alloy.* Engineering Materials, University of Sheffield. 2008.